Physiological responses of *Skeletonema costatum* to the interactions of seawater acidification and combination of photoperiod and temperature

Hangxiao Li[1,2], Tianpeng Xu[1,2], Jing Ma[1,2], Futian Li[1,2,3]* & Juntian Xu[1,2,4]*

[1]Jiangsu Key Laboratory of Marine Biotechnology, Jiangsu Ocean University, Lianyungang 222005, China
[2]Jiangsu Key Laboratory of Marine Bioresources and Environment, Jiangsu Ocean University, Lianyungang 222005, China
[3]Jiangsu Institute of Marine Resources, Lianyungang 222005, China
[4]Co-Innovation Center of Jiangsu Marine Bio-industry Technology, Jiangsu Ocean University, Lianyungang 222005, China

Correspondence to: Futian Li (futianli@jou.edu.cn) and Juntian Xu (jtxu@jou.edu.cn)

Abstract. Ocean acidification (OA), which is a major environmental change caused by increasing atmospheric CO_2, has considerable influences on marine phytoplankton. But few studies have investigated interactions of OA and seasonal changes in temperature and photoperiod on marine diatoms. In the present study, a marine diatom *Skeletonema costatum* was cultured under two different CO_2 levels (LC, 400 μatm; HC, 1000 μatm) and three different combinations of temperature and photoperiod length (8:16 L:D with 5 ℃, 12:12 L:D with 15 ℃, 16:8 L:D with 25 ℃), simulating different seasons in typical temperate oceans, to investigate the combined effects of these factors. The results showed that specific growth rate of *S. costatum* increased with increasing temperature and daylength. However, OA showed contrasting effects on growth and photosynthesis under different combinations of temperature and daylength: while positive effects of OA were observed under spring and autumn conditions, it significantly decreased growth (11 %) and photosynthesis (21 %) in winter. In addition, OA alleviated the negative effect of low temperature and short daylength on the abundance of RbcL and key photosystem II (PSII) proteins (D1 and D2). These data indicated that future ocean acidification may show differential effects on diatoms in different cluster of other factors.

Key words. diatom, growth, photosynthesis, CO_2, temperature and photoperiod

1 Introduction

Ocean acidification (OA) is one of major environmental changes caused by increasing atmospheric CO_2, which has directly raised from 280 ppm in preindustrial era to higher than 400 ppm at present (Friedlingstein et al., 2019). It is predicted that surface seawater pH would drop 0.3–0.5 and 0.5–0.7 units by the year 2100 and 2300 respectively (Caldeira and Wickett, 2003). It has been suggested that calcifying organisms, such as coral reefs and coccolithophores, are vulnerable to OA due to

the decreased calcification at elevated CO_2 (Albright et al., 2016). The responses of non-calcifying organisms such as diatoms to OA vary widely among taxonomic groups which may be detrimental, negligible or even beneficial (Gao and Campbell, 2014). Consequently, the abundance of marine phytoplankton and community structure might be altered by OA (Gattuso et al., 2015).

Diatoms are ubiquitous photosynthetic phytoplankton which account for about 20 % of global primary productivity, and thus play a crucial role in the global cycling of carbon and silicon (Falkowski et al., 2004). To overcome the limited aqueous CO_2 concentration in seawater, they have developed CO_2-concertrating mechanisms (CCMs) (Spalding, 2007). Decreased photosynthetic affinity for dissolved inorganic carbon (DIC) and activity of CCM related enzymes are generally found under increased CO_2 condition (Raven and Beardall, 2014). For phytoplankton assemblages, elevated CO_2 could lead to increases in chlorophyll *a* concentrations and the abundance of diatoms (Johnson et al., 2013). Species and strain specificity are observed in studies on physiological responses of diatoms to OA, which might be caused by the balance between positive effects of elevated CO_2 and negative effects of decreased pH (Langer et al., 2009; Li et al., 2016). In addition, acclimation and adaptation processes, i.e. the timescale of diatoms exposed to OA, could also influence the physiological effects of OA (Wu et al., 2014; Li et al., 2017). Moreover, other environmental factors, such as temperature (Seebah et al., 2014), light (Gao et al., 2012), nutrients (Li et al., 2015) and clusters of multiple factors (Xu et al., 2014a; Xu et al., 2014b), are shown to have interaction with OA on diatoms.

Diatoms are widespread across oceans, thus they would experience different photoperiods. Photoperiod controls the total light dose received by phytoplankton and thus could remarkably influence the physiological performance such as growth and lipid content of microalgae (Wahidin et al., 2013). For Antarctic sea ice microalgae *Chlamydomonas* sp., continuous illumination stimulates higher growth and nutrient absorption rates than successive darkness condition (Xu et al., 2014c). Growth rate of *Chlamydomonas reinhardtii* is gradually enhanced following the increasing photoperiod (Hsieh et al., 2018). In contrast, *Alexnadrium minutum* grows faster under short daylength relative to longer and even continuous daylength (Wang et al., 2019). Moreover, different photoperiods could influence intracellular carbon demand of microalgae, which has a stronger regulation effect on CCMs compared with effects of changes in CO_2 supply (Rost et al., 2006).

Under the combined influence of photoperiod and OA, physiological performance of phytoplankton might be different from that under single factor. For example, continuous light moderates the negative effect of OA on coccolithophore growth, although species isolated from different regions show diverse responses (Bretherton et al., 2019). The changes of photoperiod are often accompanied by increase or decrease temperature, and impacts of OA on diatoms can also be changed by temperature. For example, under OA condition, decreased metabolic activity is observed in *Phaeodactylum tricornutum* when temperature elevates (Bautista et al., 2018), while elevated temperature enhances the growth rate of *Nitzschia lecointei* (Torstensson et al., 2013).

But limited studies have investigated interactions between OA and combination of temperature and photoperiod (i.e. conditions in different seasons) on diatoms. *Skeletonema costatum* is a widespread, eurythermal and euryhaline diatom species, which frequently causes red tide. We hypothesized the effect of OA on *S. costatum* may be modulated by

photoperiod and temperature. In the present study, we investigate the physiological performance of marine diatom *Skeletonema costatum* under two different CO_2 levels and three combinations of temperature and photoperiod, which simulated different seasons in typical temperate oceans (winter, 5 ℃ with 8:16 L:D; spring or autumn, 15 ℃ with 12:12 L:D; summer, 25 ℃ with 16:8 L:D).

2 Materials and methods

2.1 Culture conditions

The diatom *Skeletonema costatum* in this study was isolated from Gaogong Island, Lianyungang, Jiangsu province (34°70′ 74.95″N, 119°49′26.47″E). Before being used in experiments, the cells were cultured in autoclaved natural seawater enriched with f / 2 medium (Guillard and Ryther, 1962). Semi-continuous cultures were maintained in 500 ml Erlenmeyer flasks with a filter unit (Millex GP, Merck, USA) in order to aerate sterile air. Triplicate independent cultures were set for each treatment at the light intensity of 150 μmol photons m^{-2} s^{-1}.

2.2 Experimental setup

In order to evaluate effects of pCO_2 levels and different combination of temperature and photoperiod on *S. costatum*, cells were cultured under winter (5 ℃ with light: dark cycle of 8:16 h), spring / autumn (15 ℃ with 12:12 h), summer (25 ℃ with 16:8 h) conditions independently with two pCO_2 levels (400 ppm, LC; 1000 ppm, HC), simulating temperature and daylength conditions of different seasons in typical temperate oceans. Temperatures and light intensity (150 μmol photons m^{-2} s^{-1}) were controlled by illumination incubators (GXZ-500B, Ningbo, China). Cells were inoculated in cultures with fresh medium which was aerated with ambient air (400 ppm) or CO_2-enriched air (1000 ppm). The high pCO_2 level was manipulated by a CO_2 plant incubator (HP 1000 G-D, Ruihua Instruments, Wuhan, China). Cultures were kept at exponential phase by diluting every 3 d, and cells concentrations were controlled below 2×10^5 cell ml^{-1} in order to minimize the effect of cell metabolism on carbonate chemistry in medium. The changes in culture pH was less than 0.05 during the 3 d (8.10 ± 0.01 for LC and 7.85 ± 0.01 for HC in winter; 8.14 ± 0.01 for LC and 7.85 ± 0.01 for HC in spring / autumn; 8.19 ± 0.02 for LC and 7.89 ± 0.02 for HC in summer). After acclimating to different treatments for at least 40 generations, following parameters were measured.

2.3 Growth measurement

To estimate the growth of *S. costatum*, triplicate samples (1 ml each) were collected from each treatment at 48 and 72 h after dilution and fixed with 10 μl Lugol's solution, then a plankton counting chamber (DSJ-01, Xundeng Instruments, Xiamen,

China) was used to count cells directly under an optical microscope (DM500, Leica, Germany). The specific growth rate was calculated as: $\mu=(\ln N_t-\ln N_0)/(t-t_0)$, where N_t represents the cell concentration (cells ml^{-1}) at time t; N_0 represents the cell concentration at time t_0, $t-t_0=1$ d. The growth rates were averaged from 3 dilution processes within each growth condition.

2.4 Chlorophyll *a* and BSi measurements

Samples were filtered onto GF / F filters (25 mm, Whatman, UK), and chlorophyll *a* were extracted with 4 ml of methanol at 4 ℃ for 24 h in darkness. An ultraviolet spectrophotometer (Ultrospect 3300 pro, Amersham Bioscience, Sweden) was used to detect the absorption values of supernatant under 632 nm, 665 nm and 750 nm after centrifuging (Biofuge primo R, Thermo, Germany). The chlorophyll *a* concentration (pg $cell^{-1}$) of *S. costatum* was calculated by the equation of Ritchie (2006).

Samples (200 ml) for biogenic silica (BSi) measurement (pmol $cell^{-1}$) were filtered onto polycarbonate filters (0.8 μm, Merck Millipore, Germany) by polysulfone filter funnel (25 mm, Pall Corporation, UK), and filters were then dried at 80 ℃ for 24 h. BSi on the filter was digested by 4 ml of 0.2 M NaOH in boiling bath for 40 min, and were neutralized with 1 ml of 1M HCl when cooled. The supernatant (1 ml) was diluted with 4 ml of Milli-Q water, and then 2 ml of molybdate soln and 3 ml of reducing agent were added into tubes. The absorption was measured at 810 nm by an ultraviolet spectrophotometer (Ultrospect 3300 pro, Amersham Bioscience, Sweden) after the color developing for 2-3 h (Brzezinski and Nelson, 1995).

2.5 Photosynthesis and respiration measurements

The net photosynthetic rate under culture condition and photosynthetic oxygen evolution rate versus light intensity (P-I) curve of *S. costatum* were measured through a Clark-type oxygen electrode (Oxygraph+, Hansatech, UK), in which temperature was controlled by a thermostatic water bath (DHX-2005, China).

For measurement of net photosynthesis under culture condition, light intensity was set as 150 μmol photons m^{-2} s^{-1} (light intensity during culture), provided by a halogen lamp (QVF135, Philips, Netherlands). Sample of 50 ml was filtered (< 0.02 MPa) onto a cellulose acetate membrane (Xinya Instruments, Shanghai, China). Cells were filtered and resuspended in 5 ml pre-aerated fresh medium under cultured condition, which was then used to determine oxygen evolution rate and cell concentration. Oxygen consumption was measured under darkness which was realized by covering an opaque box on the reaction chamber.

2.6 P-I curve measurement

For P-I curve, oxygen consumption rates in darkness and net photosynthetic oxygen evolution at 7 different light intensities (0, 10, 20, 50, 100, 200, 500, 1000 μmol photons m^{-2} s^{-1}) were identified. Light intensity was achieved by adjusting the

distance between the halogen lamp and oxygen electrode chamber. Cells were also filtered and resuspended in pre-aerated fresh medium in a similar way to photosynthesis measurement under culture condition. Photosynthetic rate and light intensity data were fitted according to Henley (1993): $P = P_m \times \tanh(\alpha \times PAR / P_m) + R_d$, where PAR is irradiance, P is photosynthetic rate, P_m is light-saturated photosynthetic rate, α is initial slope of P-I curve, R_d is dark respiration rate. I_k (saturating irradiance for photosynthesis) and I_c (light compensation point) were also calculated by: $I_k=P_m / \alpha$, $I_c=R_d / \alpha$.

2.7 Chlorophyll fluorescence measurement

Cells were concentrated by gentle vacuum filtration (< 0.02 MPa) for measurement of rapid light curves (RLCs) under 8 different PAR levels (0, 10, 20, 50, 100, 200, 500, 1000 μmol photons m^{-2} s^{-1}) lasting for 10 s each using a hand-held fluorometer (AquaPen-C AP-P 100, Chech). Relative electron transport rates (rETR) of *S. costatum* were measured, and were estimated as Wu, et al. (2010): $rETR = PAR \times Y(II) \times 0.5$, where PAR represents the photon flux density of actinic light; Y(II) represents the effective quantum yield of PSII, 0.5 is based on the assumption that PSII receives half of all absorbed quanta. RLCs were fitted as: $P = PAR / (a \times PAR^2 + b \times PAR + c)$, where P represents rETR; a, b and c are model parameters. The relative photoinhibition ratio of rETR was calculated as: $Inh(\%)=(rETR_{max}-rETR_x)/ rETR_{max} \times 100\%$, where $rETR_x$ is the value of rETR at 1000 μmol photons m^{-2} s^{-1}.

2.8 Protein measurements

The abundance of Ribulose-1,5-bisphosphate carboxylase/oxygenase (RubisCO) large subunit binding protein (RbcL) and PSII proteins (PsbA (D1), PsbD (D2), and PsbB (CP47)) were measured under different pCO_2 levels and combinations of temperature and daylength. D1 and D2 proteins are located in reaction center, while CP47 is a junction of antenna, and RbcL is a component of RubisCO which is a key enzyme in the CO_2 fixation process. For the relative value of protein measurements, cells were filtered and resuspended in 2 ml of extracting medium (50 mM Tris-HCl, pH 7.6, 5.0 mM $MgCl_2$, 10 mM NaCl, 0.4 M sucrose, and 0.1 % BSA) according to Ma et al. (2019). After cell disruption and centrifugation, supernatant liquid was used to measured chlorophyll concentration (μg ml^{-1}) according to Arnon (1949): $C = D_{652} \times 1000 \div 34.5 \times T$, where C represents total chlorophyll concentration, D_{652} represents absorption value in 652 nm, T represents dilution ratio, 1000 and 34.5 are constants. Same concentration of chlorophyll (2.4 micrograms) per lane was used for 12 % sodium dodecyl sulfate-polyacrylamide gel electrophoresis (SDS-PAGE, Mini PROTEAN, Bio-rad, America) at 150 V for 1 h, and the proteins were transferred into polyvinylidene difluoride (PVDF) membranes which were then immersed in blocking solution with antibodies (D1, D2, CP47, RbcL and Actin; Agrisera) for 1 h, and successively, goat anti-rabbit secondary antibodies were used. Blots were developed by using enhance chemluminesence luminescence (ECL) reagent and were quantified with a chemiluminescence detection system (Tanon 5500, Shanghai, China). Actin was used as internal control in order to correct the experimental error in the process of quantitative sample loading of protein, to ensure

the accuracy of the experimental results. And the data provide us with a general trend, not accurate concentrations, among different treatments.

2.9 Data analyses

Data were analyzed with IBM SPSS Statistics 24 and are presented as mean ± SD (standard deviation). One-way ANOVA was used to compare differences among combination of temperature and photoperiod treatments. The independent-samples *t*-test was applied to compare differences between two pCO_2 levels. General linear model was conducted to assess the interactive effects of CO_2 level and combination of temperature and photoperiod on growth rate, rETR, photosynthesis and respiration, contents of chlorophyll *a* and BSi and proteins. When *P* values were under 0.05, tukey test was used for *post hoc* analysis.

3 Results

3.1 Specific growth rate

Growth rate of *S. costatum* raged from 0.47 ± 0.01 to 3.22 ± 0.08 d^{-1} under different treatments and increased significantly with increasing temperature and daylength ($P < 0.05$) regardless the pCO_2 level (Fig. 1). In summer season, elevated pCO_2 showed no significant effects, however, it remarkably influenced the growth rate in other seasons. Elevated pCO_2 enhanced the growth rate by 11 % in spring and autumn ($P < 0.001$), while the reverse pattern was found in winter ($P < 0.001$). General linear model indicated that the season and CO_2 level had a notable interaction on specific growth rate ($P < 0.001$, Table 1).

3.2 Chlorophyll *a* and BSi contents

Under ambient CO_2 condition, chlorophyll *a* content was enhanced by increased temperature and daylength (Table 2), and the content was 22 % higher in summer compared with winter ($P = 0.008$). When CO_2 was elevated, chlorophyll *a* content in winter was 42 % and 32 % lower than that in spring and summer respectively ($P = 0.001$, $P = 0.004$). Elevated pCO_2 decreased chlorophyll *a* content in winter ($P = 0.022$) while enhanced it in spring ($P = 0.002$) and had no significant impact in summer. A significant interaction between season and CO_2 can be found ($P < 0.001$) (Table 1).

A different trend was detected for BSi content (Table 2). Under ambient pCO_2, BSi content decreased with higher temperature along with longer daylength and the value in winter was significantly higher than that in spring and summer ($P = 0.005$, 0.002 respectively). Higher pCO_2 decreased BSi significantly in winter ($P = 0.016$) and spring ($P = 0.007$) while had no significant influence on the content in summer ($P = 0.3$). There is a significant interaction between season and CO_2

on BSi content ($P < 0.05$) (Table 1).

3.3 Photosynthesis and respiration

Net photosynthetic oxygen evolution and dark respiration rates showed similar patterns under same CO_2 condition (Fig. 2). The lowest photosynthesis and respiration rates were observed under winter condition, and maximal rates were observed in summer at each pCO_2 level. Both photosynthesis and respiration rates increased with increasing temperature and daylength ($P < 0.05$). Elevated pCO_2 inhibited net photosynthetic rate under winter condition ($P = 0.0013$) while photosynthesis was enhanced by elevated pCO_2 in spring and autumn ($P = 0.006$). In addition, higher pCO_2 stimulated dark respiration rate in spring and autumn ($P < 0.001$). Both photosynthesis and respiration were not impacted by higher pCO_2 in summer. Interaction between season and CO_2 on net photosynthetic rate was detected ($P = 0.035$). Positive relationships of dark respiration or net photosynthetic rates and growth rate were observed (Fig. 4a, b).

3.4 P-I curve

Net photosynthetic oxygen evolution rates increased with increasing light intensity initially and then reached the plateaus in all seasons and the curves under winter condition reached the plateaus much earlier than the other two seasons (Fig. 3). Higher temperature and prolonged daylength had a main effect on P_{max}, R_d, I_k and I_c. However, elevated pCO_2 instead of season had main effect on α (Table 1). P_{max} was enhanced when temperature increasing with prolonged daylength ($P < 0.05$) except when the summer season was compared with spring and autumn condition at elevated pCO_2 (Table 3). Effects of elevated pCO_2 was only observed in spring and autumn ($P = 0.03$). I_k increased remarkably in summer under both pCO_2 treatments which was similar as R_d at elevated pCO_2 ($P < 0.05$). There was a significant interaction between CO_2 and combination of temperature and photoperiod on R_d (Table 1).

At higher pCO_2 level, $rETR_{max}$ values were significantly different among different seasons ($P < 0.05$), and the highest value was found in spring and autumn (52 % and 14% higher than winter and summer, Table 3). Elevated pCO_2 decreased $rETR_{max}$ in winter and summer ($P < 0.001$ in winter, $P = 0.01$ in summer). $rETR_{max}$ had positive correlation with growth rate when temperature and daylength increased from winter to spring / autumn condition. However, as temperature and daylength continuously increasing from spring / autumn to summer, the correlation became negative (Fig. 4c). Interactions between the two factors were detected on $rETR_{max}$ ($P < 0.001$, Table 1). Photoinhibitions were found in RLCs of cells under all treatments. As the season processed from winter to summer, photoinhibitions were alleviated significantly in both pCO_2 levels ($P < 0.05$). In spring and autumn, the inhibition at higher pCO_2 was significantly decreased compared with ambient pCO_2 condition ($P = 0.039$, Table 3).

3.5 PSII protein concentrations

The relative value of RbcL and key PSII proteins (PsbA (D1), PsbD (D2), and PsbB (CP47)) were quantified in different seasons under ambient and elevated CO_2 conditions (Fig. 5). At ambient pCO_2 level, the highest contents of all four proteins were detected in spring and autumn. Elevated pCO_2 significantly enhanced RbcL, D1 and D2 protein contents in winter ($P < 0.05$). In addition, higher pCO_2 led to increase of CP47 in summer ($P = 0.006$).

4. Discussion

Phytoplankton like diatoms have already evolved several strategies to cope with different temperature and daylength in temperate oceans, where variations of season are evident. However, the ongoing elevated pCO_2 combining with changes in temperature and daylength is a new stress on diatoms and we know little about their interactions. Therefore, we examined the combined effects of pCO_2 and seasonal changes in temperature and photoperiod on the physiological performance of a typical marine diatom *S. costatum*.

4.1 Physiological responses of *S. costatum* to different combinations of temperature and photoperiod

In the present study, the growth rate of *S. costatum* increased with increasing temperature and daylength regardless of the pCO_2 level (Fig. 1). Previous studies showed that most phytoplankton, such as *Chlamydomonas reinhardtii*, *Trichodesmium* or *Alexandrium catenella*, grew faster under prolonged photoperiods (Cai and Gao, 2015) although *Alexnadrium minutum* grew faster under shorter photoperiods (Wang et al., 2019). For *S. costatum*, a remarkably higher contribution of HCO_3^- to the overall carbon uptake was observed under light dark cycles compared with continuous light, and a shorter photoperiod led to lower photosynthetic affinity for inorganic carbon (Rost et al., 2006). Basically, the Chl *a* quota in microalgae increases with decreasing daylength, however, our results exhibited inverse pattern (Table 2). The inconsistency might be caused by the different temperatures set in studies, which is another main environmental factor affecting the growth of diatoms.

Increasing temperature may lead to various changes in growth rate depending on whether the temperature is optimal for the species. For *S. costatum*, its growth rate has been shown to increase with temperature up to 30 ℃ (Ebrahimi and Salarzadeh, 2016). Zhang et al. (2020) also found that the growth rate of *S. costatum* could increase with temperature from 5 ℃ to 30 ℃ and then drop sharply. The underlying mechanism is that elevated temperature promotes *S. costatum* metabolic rates when nutrients are abundant. This could be shown by the relationship between respiration and growth. Higher mitochondrial respiration can result in higher growth rate theoretically (Geider and Osborne, 1989), since this process provides ATP and carbon skeletons (Raven et al., 2017). It seems that temperature shows the dominant effect compared with daylength.

Rubisco is an important enzyme for carbon fixation, psychrophilic diatoms utilize increasing abundance of RbcL protein to maintain high cellular enzymatic rates and growth rate at low temperature (Young et al., 2015). However, for diatoms in temperate area, the amount of RbcL protein decreased in low temperature along with short daylength compared with higher

temperature and longer daylength in our results. Low abundance of RbcL was in line with slower growth rate in winter condition.

4.2 Effect of ocean acidification under different seasons

Our results showed that the impacts of elevated pCO_2 on *S. costatum* depended on seasonal changes in temperature and photoperiod. High pCO_2 had enhanced the growth of *S. costatum* in spring / autumn and reduced it in winter, while no significant effects were detected in summer (Fig. 1). CO_2 concentration mechanisms (CCMs) is energy-dependent and high pCO_2 down-regulate CCMs of most phytoplankton including *S. costatum*, so the saved energy could be used for growth (Raven et al., 2017). Higher initial slope of the P-I curve at elevated pCO_2 might be partly responsible for the higher growth rate compared with that at ambient pCO_2 (Table 3). But in winter, growth decreased under OA condition, although respiration and P_{max} in P-I curves had no significant changes. This is because the combination of biochemical and biophysical CCMs may cause the lack of a positive response to elevated pCO_2 under near-optimal growth conditions (Passow, 2015). In addition, when other environmental factors are stressful, the sensitivity of diatoms to CO_2 and temperature is prominent (Taucher et al., 2015). The shorter daylength and low temperature simulating winter condition in present study can be seen as stressors, under which *S. costatum* was more sensitive to elevated pCO_2. When temperature and photoperiod are optimal, positive or neutral effects of higher pCO_2 were observed. However, different patterns were reported for other species, such as *E. huxleyi* and the macroalgae *Ulva linza* (Bretherton et al., 2019; Yue et al., 2019). For these two species, reduced growth rate at elevated pCO_2 were found when the daylength was longest. High temperature might accelerate nutrient uptake and metabolic rates, which may alleviate the negative effects of longer daylength under higher pCO_2 environment (Bretherton et al., 2019; Yue et al., 2019). Maximum photosynthetic rate increased significantly under higher pCO_2 in spring and autumn condition. This was consistent with the higher photosynthetic efficiency and growth rate (Table 3, Fig. 1).

Silicification directly relates to cell division and growth, and is independent of photoperiod (Brzezinski, 1992). BSi contents generally increased with decreasing growth rate when any limiting factors such as temperature, light or ammonium exist (Martin et al., 2000). In the present study, elevated pCO_2 mitigated the negative effects of temperature and photoperiod limitation on BSi content (Table 2). Higher BSi contents in winter under ambient CO_2 condition can intensify the ballasting effects and thus impact the sinking rate of organic matters produced by diatoms.

Lavaud et al. (2016) indicated that PSII activity and phosphorylation of thylakoid protein may play a crucial role in controlling the change of the photosynthetic activity. The contents of D1 and D2 proteins decreased in winter because of the negative effect of lower temperature (Mock & Valentin, 2004), while elevated pCO_2 level increased their contents (Fig. 5). The protein contents included both photochemically active PSII, and those PSII which are inactivated but retain D1 and D2 subunits (Li et al., 2015). Proteins will be degraded and synthesized rapidly after damage. However, the degraded rate of photosynthetic proteins from photoinactivated PSII complexes could be different according to culture condition. For example,

the removal rate of D1 protein increased with growth light in the diatom *Thalassiosira pseudonana* (Campbell et al., 2013). Therefore, the photosynthetic rate might decouple with the contents of proteins. The decline in growth under winter condition might result from the increased metabolic costs of photoprotection and elevated D1 turnover under the combination of short daylength limitation and low temperature (Hoppe et al., 2015). Although RbcL decreased with elevated CO_2 in some studies that might be caused by the decrease in RuBP concentration for diatoms (Endo et al., 2015), McCarthy et al. (2012) observed an increase in Rubisco concentration with higher CO_2, which is in line with the present study under winter condition. Light and temperature could affect RbcL amount in phytoplankton. RbcL increased slightly with higher CO_2 at low light intensity condition, while it decreased slightly at higher light intensity in the research of Levitan et al. (2010). In the present study, the combination of low temperature and short daylength might lead to a complex trend of RbcL, elevated CO_2 might stimulate the sensitivity of *S. costatum* to low temperature which lead to a steep rise of RbcL in winter.

For diatoms, a mounting body of studies has pay attention to the effect of interactions of ocean acidification and other environmental factors such as light intensity, UV, temperature, nutrient limitation, salinity or photoperiod (Gao et al., 2012; Yue et al., 2019), and the results showed positive, negative or neutral effects (Xu et al., 2014c; Li et al., 2017). However, few studies combined elevated pCO_2 with seasonal changes in seawater physical and chemical characters on marine diatoms. In this study, temperature and photoperiod were chosen as seasonal factors to investigate the combined effects of pCO_2 and these two factors on physiology of *S. costatum*. Our results suggested temperature and photoperiod could mediate effects of elevated pCO_2 on the typical diatom *S. costatum*. Positive effects of OA on growth and photosynthesis were observed in spring and autumn, while negative effects were found in winter condition. To better understand how global climate changes would affect marine diatoms in the future, it is necessary to explore the interactive effects of ocean acidification with seasonal changes in seawater characters.

Author Contributions

JX and FL conceived and designed the experiments; HL and TX carried out the experiments; HL, FL and JX analyzed data; HL wrote the draft of the paper; FL, JM and JX revised the manuscript and approved this version for submission.

Competing interests

The authors declare that they have no conflict of interest.

Acknowledgements

This study was funded by China Postdoctoral Science Foundation (2019M661766), the Six Talents Peaks in Jiangsu Province (JY-086), Postgraduate Research & Practice Innovation Program of Jiangsu Province (KYCX19_2290), the Priority

Academic Program Development of Jiangsu Higher Education Institutions.

References

Albright, R., Caldeira, L., Hosfelt, J., Kwiatkowski, L., Maclaren, K. J., Mason, B., Nebuchina, Y., Ninokawa, A., Pongratz, J., Ricke, K. L., Rivlin, T., Schneider, K., Sesboue, M., Shamberger, K. E. F., Silverman, J., Wolfe, K., Zhu, K., and Caldeira K.: Reversal of ocean acidification enhances net coral reef calcification, Nature, 531, 362–365, doi: 10.1038/nature17155, 2016.

Arnon D. I.: Copper enzymes in isolated chloroplasts. Polyphenoloxidase in *Beta vulgaris*, Plant Physiol., 24, 1–15, doi: 10.1104/pp.24.1.1, 1949.

Bautistachamizo, E., Sendra, M., Cid, A., Seoane, M., Orte, M. R. D., and Riba, I.: Will temperature and salinity changes exacerbate the effects of seawater acidification on the marine microalga *Phaeodactylum tricornutum*? Sci. Total Environ., 634, 87–94, doi: 10.1016/j.scitotenv.2018.03.314, 2018.

Behrenfeld, M. J., Prasil, O., Kolber, Z., Babin, M., and Falkowski, P.: Compensatory changes in Photosystem II electron turnover rates protect photosynthesis from photoinhibition, Photosyn. Res., 58, 259–268, doi: 10.1023/A:1006138630573, 1998.

Bretherton, L., Poulton, A. J., Lawson, T., Rukminasari, N., Balestreri, C., Schroeder, D. C., Moore, C. M., and Suggett, D. J.: Day length as a key factor moderating the response of coccolithophore growth to elevated pCO_2, Limnol. Oceanogr., 64, 1284–1296, doi: 10.1002/lno.11115, 2019.

Brzezinski, M. A., and Nelson, D. M.: The annual silica cycle in the Sargasso Sea near Bermuda, Deep Sea Research Part I: Oceanographic Research Papers, 42, 1215–1237, doi: 10.1016/0967-0637(95)93592-3, 1995.

Cai, X., and Gao, K.: Levels of daily light doses under changed day-night cycles regulate temporal segregation of photosynthesis and N_2 fixation in the Cyanobacterium *Trichodesmium erythraeum* IMS101, PloS One, 10, e0135401, doi: 10.1371/journal.pone.0135401, 2015.

Caldeira, K., and Wickett, M. E.: Oceanography: anthropogenic carbon and ocean pH, Nature, 425, 365–365, doi: 10.1038/425365a, 2003.

Campbell, D. A., Hossain, Z., Cockshutt, A. M., Zhaxybayeva, O., Wu, H. and Li, G.: Photosystem II protein clearance and FtsH function in the diatom *Thalassiosira pseudonana*. Photosyn. Res., 115, 43–54, doi: 10.1007/s11120-013-9809-2, 2013.

Chen, X., and Gao, K.: Characterization of diurnal photosynthetic rhythms in the marine diatom *Skeletonema costatum* grown in synchronous culture under ambient and elevated CO_2, Funct. Plant Biol., 31, 399–404, doi: 10.1071/FP03240, 2004.

Ebrahimi, E., and Salarzadeh, A.: The effect of temperature and salinity on the growth of *Skeletonema costatum* and *Chlorella capsulata* in vitro, International Journal of Life Sciences, 10, 40–44, doi: 10.3126/ijls.v10i1.14508, 2016.

Eilers, P. H. C. and Petters, J. C. H.: A model for the relationship between light intensity and the rate of photosynthesis in phytoplankton, Ecol. Modell., 42, 199–215, doi: 10.1016/0304-3800(88)90057-9, 1988.

Endo, H., Sugie, K., Yoshimura, T., and Suzuki, K.: Effects of CO_2 and iron availability on *rbcL* gene expression in Bering Sea diatoms, Biogeosciences, 12, 2247–2259, doi: 10.5194/bg-12-2247-2015, 2015.

Falkowski, P. G., Katz, M. E., Knoll, A. H., Quigg, A., Raven, J. A., Schofield, O., and Taylor, F. J. R.: The evolution of modern eukaryotic phytoplankton, Science, 305, 354–360, doi: 10.1126/science.1095964, 2004.

Friedlingstein P, Jones M W, Osullivan M, Andrew, R. M., Hauck, J., Peters, G. P., Peters, W., Pongratz, J., Sitch, S., Quere, C. L., Bakker, D. C. E., Canadell, J. G., Ciais, P., Jackson, R. B., Anthoni, P., Barbero, L., Bastos, A., Bastrikov, V., Becker, M., Bopp, L., Buitenhuis, E. T., Chandra, N., Chevallier, F., Chini, L. P., Currie, K. I., Feely, R. A., Gehlen, M., Gilfillan, D., Gkritzalis, T., Goll, D., Gruber, N., Gutekunst, S., Harris, I., Haverd, V., Houghton, R. A., Hurtt, G. C., Ilyina, T., Jain, A. K., Joetzjer, E., Kaplan, J. O., Kato, E., Goldewijk, K. K., Korsbakken, J. I., Landschutzer, P., Lauvset, S. K., Lefevre, N., Lenton, A., Lienert, S., Lombardozzi, D., Marland, G., Mcguire, P. C., Melton, J. R., Metzl, N., Munro, D. R., Nabel, J. E. M. S., Nakaoka, S. I., Neill, C., Omar, A. M., Ono, T., Peregon, A., Pierrot, D., Poulter, B., Rehder, G., Resplandy, L., Robertson, E., Rodenbeck, C., Seferian, R., Schwinger, J., Smith, N., Tans, P. P., Tian, H., Tilbrook, B., Tubiello, F. N., Werf, G. R. V. D., Wiltshire, A., Zaehle, S.: Global carbon budget 2019, Earth Syst. Sci. Data, 11, 1783–1838, doi: 10.5194/essd-11-1783-2019, 2019.

Gao, G., Xia, J., Yu, J., Fan, J., and Zeng, X.: Regulation of inorganic carbon acquisition in a red tide alga (*Skeletonema costatum*): the importance of phosphorus availability, Biogeosciences, 15, 4871–4882, doi: 10.5194/bg-15-4871-2018, 2018.

Gao, K., and Campbell, D. A.: Photophysiological responses of marine diatoms to elevated CO_2 and decreased pH: a review, Funct. Plant Biol., 41, 449–459, doi: 10.1071/FP13247, 2014.

Gao, K., Xu, J., Gao, G., Li, Y., Hutchins, D. A., Huang, B., Wang, L., Zheng, Y., Jin, P., Cai, X., Hader, D., Li, W., Xu, K., Liu, N., and Riebesell, U.: Rising CO_2 and increased light exposure synergistically reduce marine primary productivity, Nat. Clim. Chang., 2, 519–523, doi: 10.1038/NCLIMATE1507, 2012.

Gattuso, J. P., Magnan, A., Bille, R., Cheung, W., Howes, E. L., Joos, F., Allemand, D., Bopp, L., Cooley, S. R., Eakin, C. M., Hoeghguldberg, O., Kelly, R. P., Portner, H., Rogers, A. D., Baxter, J. M., Laffoley, D., Osborn, D., Rankovic, A., Rochette, J., Sumaila, U. R., Treyer, S., and Turley, C. M.: Contrasting futures for ocean and society from different anthropogenic CO_2 emissions scenarios, Science, 349, aac4722, doi: 10.1126/science.aac4722, 2015.

Geider, R. J., and Osborne, B. A.: Respiration and microalgal growth: a review of the quantitative relationship between dark respiration and growth, New Phytol., 112, 327–341, doi: 10.1111/j.1469-8137. 1989. Tb00321.x, 1989.

Guillard, R. R. L., and Ryther, J. H.: Studies of marine planktonic diatoms: I. *Cyclotella nana* Hustedt, and *Detonula confervacea* (Cleve) Gran, Can. J. Microbiol., 8, 229–239, doi: 10.1139/m62-029, 1962.

Hartmann, J., West, A. J., Renforth, P., Kohler, P., Rocha, C. L. D. L., Wolfgladrow, D., Durr, H. H., and Scheffran, J.: Enhanced chemical weathering as a geoengineering strategy to reduce atmospheric carbon dioxide, supply nutrients, and

mitigate ocean acidification, Rev. Geophys., 51, 113–149, doi: 10.1002/rog.20004, 2013.

Henley, W. J.: Measurement and interpretation of photosynthetic light-response curves in algae in the context of photoinhibition and diel changes, J. Phycol., 29, 729–739, doi: 10.1111/j.0022-3646.1993.00729.x, 1993.

Hoppe, C. J. M., Holtz, L. M., Trimborn, S., and Rost, B.: Ocean acidification decreases the light-use efficiency in an Antarctic diatom under dynamic but not constant light, New Phytol., 207, 159–171, doi: 10.1111/nph.13334, 2015.

Johnson, V. R., Brownlee, C., Rickaby, R. E. M., Graziano, M., Milazzo, M., and Hallspencer, J. M.: Responses of marine benthic microalgae to elevated CO_2, Mar. Biol., 160, 1813–1824, doi: 10.1007/s00227-011-1840-2, 2013.

Langer, G., Nehrke, G., Probert, I., Ly, J., and Ziveri, P.: Strain-specific responses of *Emiliania huxleyi* to changing seawater carbonate chemistry, Biogeosciences, 6, 2637–2646, doi: 10.5194/bg-6-2637-2009, 2009.

Lavaud, J., Six, C., and Campbell, D. A.: Photosystem II repair in marine diatoms with contrasting photophysiologies, Photosyn. Res., 127, 189–199, doi: 10.1007/s11120-015-0172-3, 2016.

Levitan, O., Kranz, S. A., Spungin, D., Prášil, O., Rost, B., and Berman-Frank, I.: Combined effects of CO_2 and light on the N_2-fixing Cyanobacterium *Trichodesmium* IMS101: a mechanistic view. Plant Physiol., 154, 346–356, doi: https://doi.org/10.1104/pp.110.159285, 2010.

Li, F., Beardall, J., Collins, S., and Gao, K.: Decreased photosynthesis and growth with reduced respiration in the model diatom *Phaeodactylum tricornutum* grown under elevated CO_2 over 1800 generations, Glob. Chang. Biol., 23, 127–137, doi: 10.1111/gcb.13501, 2017.

Li, F., Beardall, J., and Gao, K.: Diatom performance in a future ocean: interactions between nitrogen limitation, temperature, and CO_2-induced seawater acidification, ICES J. Mar. Sci., 75, 1451–1464, doi: 10.1093/icesjms/fsx239, 2018.

Li, F., Wu, Y., Hutchins, D. A., Fu, F., and Gao, K.: Physiological responses of coastal and oceanic diatoms to diurnal fluctuations in seawater carbonate chemistry under two CO_2 concentrations, Biogeosciences, 13, 6247–6259, doi: 10.5194/bg-2016-281, 2016.

Li, G., Brown, C. M., Jeans, J. A., Donaher, N., A., McCarthy, A. and Campbell, D., A.: The nitrogen costs of photosynthesis in a diatom under current and future pCO_2, New Phytol., 205, 533–543, doi: 10.1111/nph.13037, 2015.

Li, W., Gao, K., and Beardall, J.: Interactive effects of ocean acidification and nitrogen-limitation on the diatom *Phaeodactylum tricornutum*, PLoS One, 7, e51590, doi: 10.1371/journal.pone.0051590, 2012.

Li, W., Gao, K., and Beardall J.: Nitrate limitation and ocean acidification interact with UV-B to reduce photosynthetic performance in the diatom *Phaeodactylum tricornutum*, Biogeosciences, 12, 2383–2393, doi: 10.5194/bg-12-2383-2015, 2015.

Ma, J., Wang, W., Liu, X., Wang, Z., Gao, G., Wu, H., Li, X., and Xu, J.: Zinc toxicity alters the photosynthetic response of red alga *Pyropia yezoensis* to ocean acidification, Environ. Sci. Pollut. Res., 27, 3202–3212, doi: 10.1007/s11356-019-06872-7, 2020.

Malviya, S., Scalco, E., Audic, S., Vincent, F., Veluchamy, A., Poulain, J., Wincker, P., Iudicone, D., Vargas, C. D., Bittner, L., Zingone, A., and Bowler, C.: Insights into global diatom distribution and diversity in the world's ocean, Proc. Natl. Acad.

Sci., 113, E1516–E1525, doi: 10.1073/pnas.1509523113, 2016.

Martin-Je´ze´quel, V., Hildebrand, M. and Brzezinski, M. A.: Silicon metabolism in diatoms: implications for growth, J. Phycol., 36, 821–840, doi: 10.1046/j.1529-8817. 2000. 00019. x, 2000.

McCarthy, A., Rogers, S. P., Duffy, S. J., and Campbell, D. A.: Elevated carbon dioxide differentially alters the photophysiology of *Thalassiosira Pseudonana* (bacillariophyceae) and *Emiliania Huxleyi* (haptophyta)[1], J. Phycol., 48, 635–646, doi: https://doi.org/10.1111/j.1529-8817.2012.01171.x, 2012.

Meyers, M. T., Cochlan, W. P., and Carpenter, E. J.: Effect of ocean acidification on the nutritional quality of marine phytoplankton for copepod reproduction, PloS One, 14, e0217047, doi: 10.1371/journal.pone.0217047, 2019.

Mock, T., Valentin, K.: Photosynthesis and cold acclimation: molecular evidence from a polar diatom[1], J. Phycol., 40, 732–741, doi: 10.1111/j.1529-8817.2004.03224.x, 2004.

Passow, U., and Laws, E. A.: Ocean acidification as one of multiple stressors: growth response of *Thalassiosira weissflogii* (diatom) under temperature and light stress, Mar. Ecol. Prog. Ser., 541, 75–90, doi: 10.3354/meps11541, 2015.Raven, J. A., and Beardall, J.: CO_2 concentrating mechanisms and environmental change, Aquat. Bot., 118, 24–37, doi: 10.1016/j.aquabot.2014.05.008, 2014.

Raven, J. A., Beardall, J., and Sánchez-Baracaldo, P.: The possible evolution and future of CO_2-concentrating mechanisms, J. Exp. Bot., 68, 3701–3716, doi: 10.1093/jxb/erx110, 2017.

Raven, J. A., and Johnston, A. M.: Mechanisms of inorganic-carbon acquisition in marine phytoplankton and their implications for the use of other resources, Limnol. Oceanogr., 36, 1701–1714, doi: 10.4319/lo.1991.36.8.1701, 1991.

Ritchie, R. J.: Consistent sets of spectrophotometric chlorophyll equations for acetone, methanol and ethanol solvents, Photosyn.Res., 89, 27–41, doi: 10.1007/s11120-006-9065-9, 2006.

Rost, B., Riebesell, U., and Sültemeyer, D.: Carbon acquisition of marine phytoplankton: effect of photoperiod length, Limnol. Oceanogr., 51, 12–20, doi: 10.4319/lo.2006.51.1.0012, 2006.

Seebah, S., Fairfield, C., Ullrich, M. S., and Passow, U.: Aggregation and sedimentation of *Thalassiosira weissflogii* (diatom) in a warmer and more acidified future ocean, PloS One, 9, e112379, doi: 10.1371/journal.pone.0112379, 2014.

Spalding, M. H.: Microalgal carbon-dioxide-concentrating mechanisms: Chlamydomonas inorganic carbon transporters, J. Exp. Bot., 59, 1463–1473, doi: 10.1093/jxb/erm128, 2007.

Taucher, J., Jones, J., James, A., Brzezinski, M. A., Carlson, C. A., Riebesell U., and Passow, U.: Combined effects of CO_2 and temperature on carbon uptake and partitioning by the marine diatoms *Thalassiosira weissflogii* and *Dactyliosolen fragilissimus*, Limnol. Oceanogr., 60, 901–919, doi: 10.1002/lno.10063, 2015.

Torstensson, A., Hedblom, M., Andersson, J., Andersson. M. X., and Wulff, A.: Synergism between elevated pCO_2 and temperature on the Antarctic sea ice diatom *Nitzschia lecointei*, Biogeosciences, 10, 6391–6401, doi: 10.5194/bg-10-6391-2013, 2013.

Wahidin, S., Idris, A., and Shaleh, S. R. M.: The influence of light intensity and photoperiod on the growth and lipid content of microalgae *Nannochloropsis* sp., Bioresour. Technol., 129, 7–11, doi: 10.1016/j.biortech.2012.11.032, 2013.

Wang, H., Zhang, B., Song, X., Jian, X. Tang, C. Campbell, D. A. Lin, Q., and Li, G.: High antioxidant capability interacts with respiration to mediate two *Alexandrium* species growth exploitation of photoperiods and light intensities, Harmful Algae, 82, 26–34, doi: 10.1016/j.hal.2018.12.008, 2019.

Wu, Y., Campbell, D. A., Irwin, A. J., Suggett, D. J., and Finkel, Z. V.: Ocean acidification enhances the growth rate of larger diatoms, Limnol. Oceanogr., 59, 1027–1034, doi: 10.4319/lo.2014.59.3.1027, 2014.

Xu, K., Fu, F., and Hutchins, D. A.: Comparative responses of two dominant Antarctic phytoplankton taxa to interactions between ocean acidification, warming, irradiance, and iron availability, Limnol. Oceanogr., 59, 1919–1931, doi: 10.4319/lo.2014.59.6.1919, 2014a.

Xu, J., Gao, K., Li, Y., and Hutchins, D. A.: Physiological and biochemical responses of diatoms to projected ocean changes, Mar. Ecol. Prog. Ser., 515, 73–81, doi: 10.3354/meps11026, 2014b.

Xu, D., Wang, Y., Fan, X., Wang, D., Ye, N., Zhang, X., Mou, S., Guan, Z., and Zhuang, Z.: Long-term experiment on physiological responses to synergetic effects of ocean acidification and photoperiod in the Antarctic sea ice algae *Chlamydomonas sp.* ICE-L, Environ. Sci. Technol., 48, 7738–7746, doi: 10.1021/es404866z, 2014c.

Young, J. N., Goldman, J. A. L., Kranz, S. A., Tortell, P. D., and Morel, F. M. M.: Slow carboxylation of Rubisco constrains the rate of carbon fixation during Antarctic phytoplankton blooms, New Phytol., 205, 172–181, doi: 10.1111/nph.13021, 2015.

Yue, F., Gao, G., Ma, J., Wu, H., Li, X., and Xu, J.: Future CO_2-induced seawater acidification mediates the physiological performance of a green alga *Ulva linza* in different photoperiods, PeerJ, 7, e7048, doi: 10.7717/peerj.7048, 2019.

Zhang. L., Li, H., Wu, M., Li, F., and Xu, J.: Effects of seawater acidification on photosynthetic physiological characteristics of *Skeletonema costatum* at different temperatures, J. Ocean Univ. China, 29, 1–7, doi: 10.3969/j.issn.2096-8248.2020.01.001, 2020.

Table 1: Significance test results of growth, BSi, photosynthetic and respiration rates, parameters of P-I (P_{max} is the maximum net photosynthetic rate, α is the photosynthetic efficiency, R_d is the dark respiration rate) and RLCs curves ($rETR_{max}$, which is the maximum relative electron rate) for combination of temperature and photoperiod (season), CO_2, and their interactions.

Parameter	Season		CO_2		Season * CO_2	
	F	*p*	F	*p*	F	*p*
Specific growth rate	7662.1	**≤0.001**	0.3	0.569	27.3	**≤0.001**
BSi	22.6	**≤0.001**	22.5	**≤0.001**	10.9	**≤0.001**
Photosynthesis	452.1	**≤0.001**	0.1	0.735	4.5	**0.0345**
Dark respiration	51.9	**≤0.001**	7.6	**0.018**	1.9	0.182
P_{max}	85.5	**≤0.001**	6.3	**0.028**	3.4	0.069
α	1.8	0.211	6.2	**0.028**	1.5	0.262
R_d	7.3	**0.010**	3.3	0.097	4.2	**0.044**
$rETR_{max}$	85.3	**≤0.001**	98.5	**≤0.001**	26.0	**≤0.001**

Table 2: Chl *a* (pg cell^{-1}) and BSi (pmol cell^{-1}) contents of *S. costatum* acclimated to ambient and elevated pCO_2 in different seasons. The data are mean ± SD values of triplicate cultures (n = 3). Different lowercases represent significant differences ($P < 0.05$) between two CO_2 levels under same season (*t*-test).

Treatments	Chl *a*		BSi	
	LC	HC	LC	HC
Winter	0.18 ± 0.008^a	0.15 ± 0.013^b	0.035 ± 0.003^a	0.025 ± 0.003^b
Spring / Autumn	0.19 ± 0.007^a	0.26 ± 0.014^b	0.025 ± 0.002^a	0.019 ± 0.001^b
Summer	0.22 ± 0.015^a	0.23 ± 0.024^a	0.023 ± 0.001^a	0.024 ± 0.002^a

Table 3: Photosynthetic parameters fitted from $P_{(O2)}$-I and rapid light curves for *S. costatum* acclimated to ambient and elevated pCO_2 in different seasons. P_{max} (pmol O_2 cell^{-1} h^{-1}) is the maximum net photosynthetic rate, α is the photosynthetic efficiency, R_d (pmol O_2 cell^{-1} h^{-1}) is the dark respiration rate, I_k (μmol photons m^{-2} s^{-1}) is the photosynthetic saturated light intensity, I_c (μmol photons m^{-2} s^{-1}) is light compensation point, $rETR_{max}$ is the maximum relative electron rate and Inh is the relative photoinhibition ratio of rETR. Different lowercases represent significant differences ($P < 0.05$) between two CO_2 levels under same season (*t*-test).

	P_{max}	α(O_2)	R_d	I_k(O_2)	I_c	I_k (ETR)	α (ETR)	$rETR_{max}$	Inh (%)
Winter-LC	0.13 ± 0.01^a	0.0012 ± 0.00007^a	0.011 ± 0.006^a	112.4 ± 17.3^a	9.8 ± 5.1^a	302.7 ± 8.3^a	0.21 ± 0.008^a	59.0 ± 1.76^a	147.3 ± 6.7^a
Winter-HC	0.11 ± 0.02^a	0.0012 ± 0.00045^a	0.003 ± 0.002^a	97.5 ± 21.7^a	7.2 ± 3.3^a	193.6 ± 10.7^b	0.22 ± 0.005^a	40.3 ± 1.43^b	135.0 ± 16.8^a
Spring-LC	0.23 ± 0.04^a	0.0011 ± 0.00012^a	0.007 ± 0.003^a	204.1 ± 28.0^a	5.7 ± 1.9^a	373.0 ± 8.5^a	0.20 ± 0.0005^a	67.4 ± 1.59^a	68.7 ± 6.9^a
Spring-HC	0.31 ± 0.03^b	0.0016 ± 0.00019^b	0.019 ± 0.007^a	192.3 ± 19.9^a	11.1 ± 3.5^a	386.6 ± 10.2^a	0.21 ± 0.005^b	61.6 ± 3.77^a	54.5 ± 4.3^b
Summer-LC	0.35 ± 0.05^a	0.0011 ± 0.00009^a	0.016 ± 0.008^a	336.7 ± 66.3^a	14.5 ± 7.1^a	465.1 ± 18.6^a	0.12 ± 0.018^a	57.1 ± 0.04^a	28.9 ± 4.3^a
Summer-HC	0.41 ± 0.05^a	0.0013 ± 0.00018^a	0.032 ± 0.011^a	322.8 ± 36.1^a	25.4 ± 10.5^a	462.3 ± 16.8^a	0.16 ± 0.009^b	53.8 ± 1.29^b	27.1 ± 2.7^a

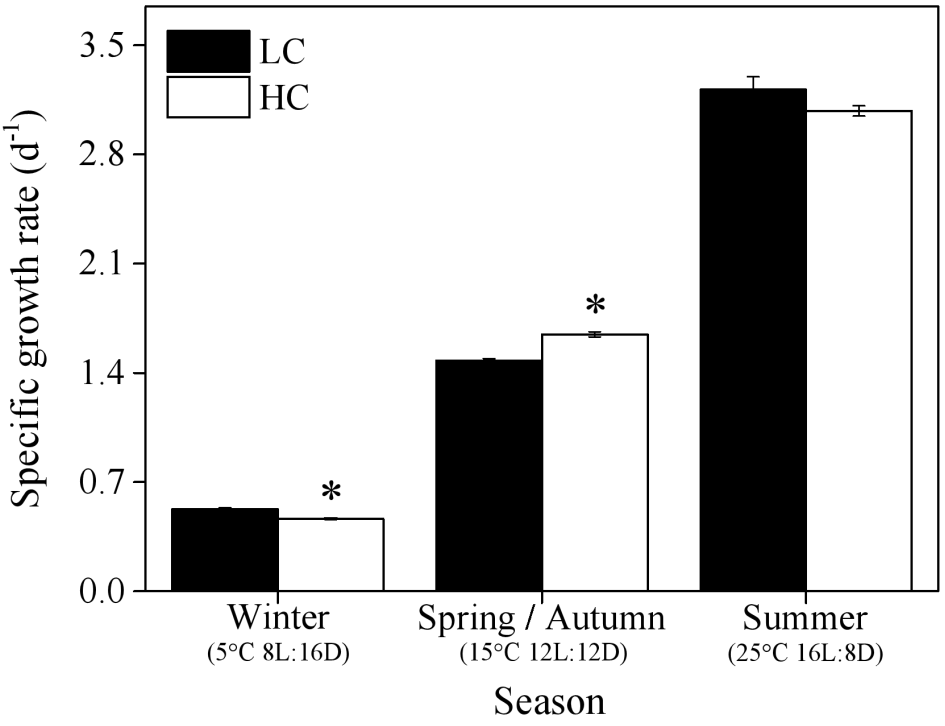

465

Figure 1: Specific growth rate of *S. costatum* acclimated to ambient (LC, black bars) and elevated pCO_2 (HC, white bars) under different combination of temperature and photoperiod conditions. The data are mean ± SD values of triplicate cultures (n = 3). Asterisks represent significant differences ($P < 0.05$) between two CO_2 levels under same season condition (*t*-test).

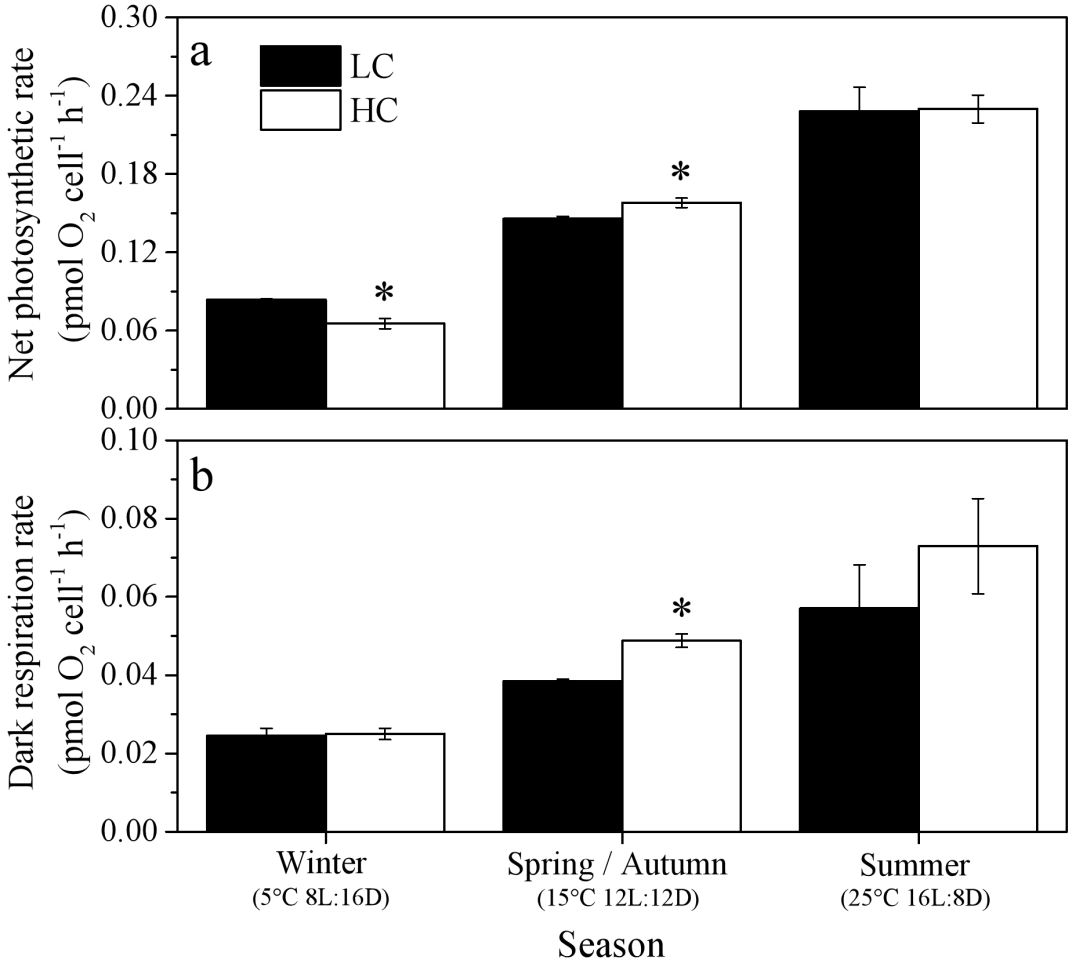

Figure 2: Net photosynthetic (a) and dark respiration rates (b) of *S. costatum* acclimated to ambient (LC, black bars) and elevated pCO_2 (HC, white bars) under different combination of temperature and photoperiod conditions. The data are mean ± SD values of triplicate cultures (n = 3). Asterisks represent significant differences ($P < 0.05$) between two CO_2 levels under same season condition (*t*-test).

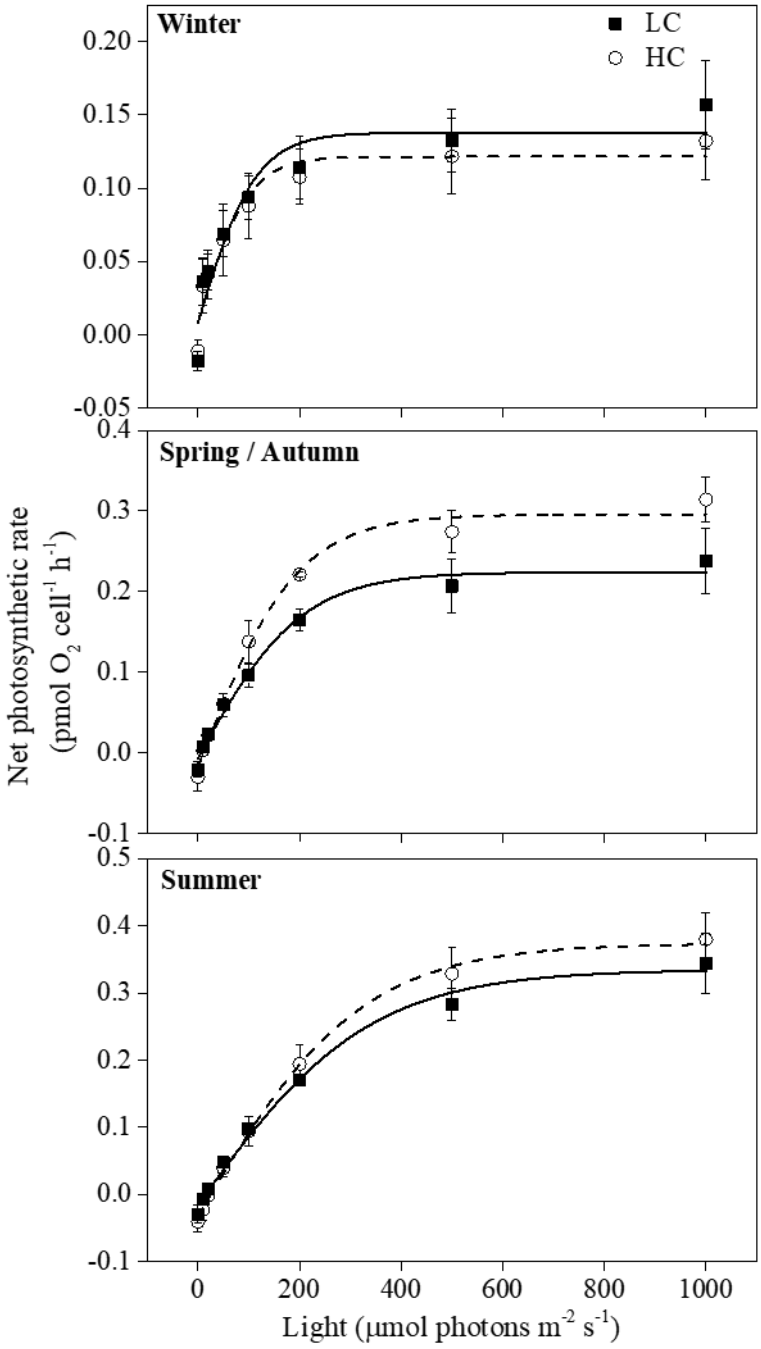

Figure 3: Photosynthesis-light curves (P-I curves) of cells acclimated to ambient and elevated pCO_2 in different seasons. The data are mean ± SD values of triplicate cultures (n = 3).

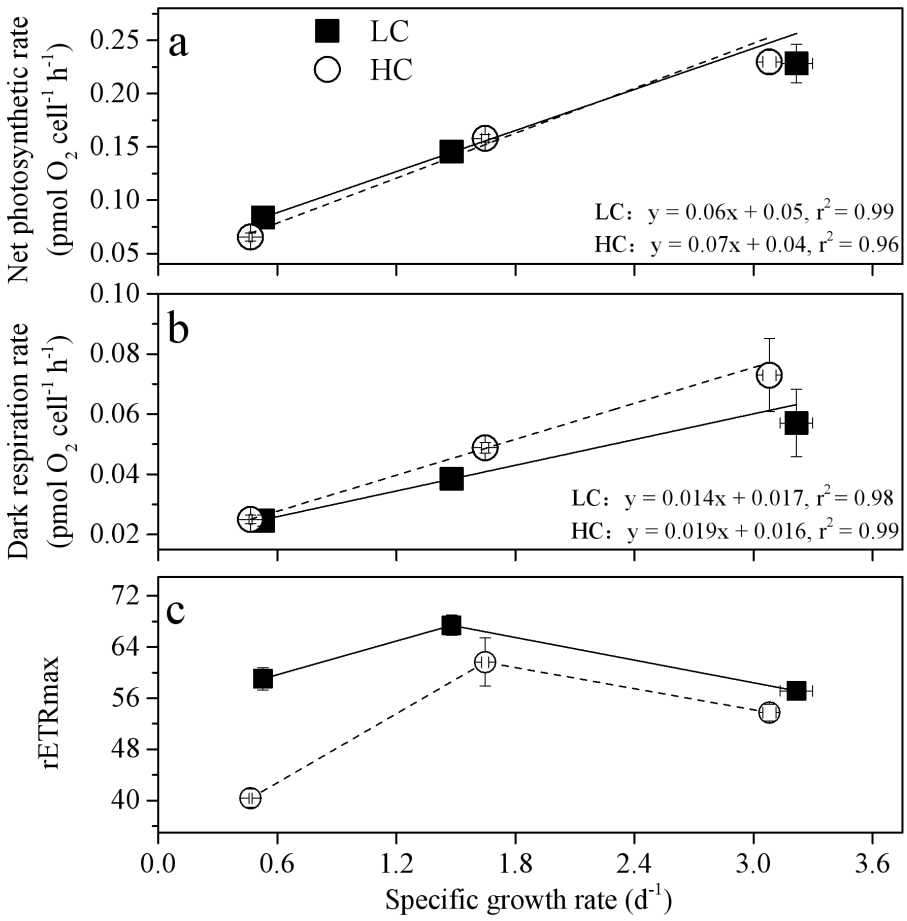

Figure 4: The relationship between net photosynthetic rate (a), dark respiration (b), $rETR_{max}$ (c) and specific growth rate of *S. costatum* acclimated to ambient (LC, black square) and elevated pCO_2 (HC, white circle) under different combination of temperature and photoperiod conditions. The data are mean ± SD values of triplicate cultures (n = 3).

485

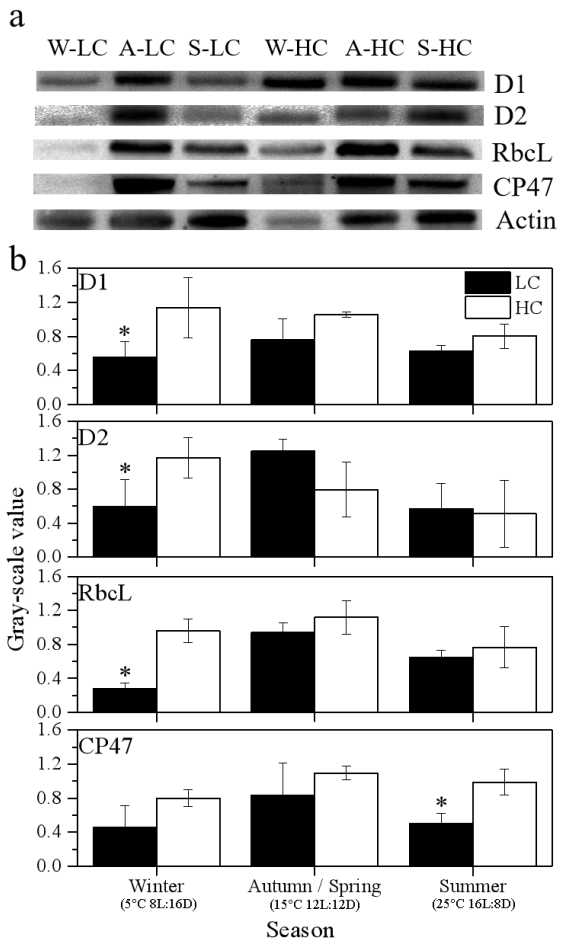

Figure 5: (a) Immunoblot using antibodies against RbcL and key PSII proteins (PsbA (D1), PsbD (D2), and PsbB (CP47)) isolated from *S. costatum* acclimated to ambient and elevated pCO_2 in different season levels (W for winter, A for autumn, S for summer). Each line was loaded with similar amounts of proteins. (b) Quantitative analysis of proteins. The relative abundance of each band was estimated by densitometric scanning of the exposed films. Asterisks represent significant differences ($P < 0.05$) between two CO_2 levels under same season (*t*-test).